



ISSN NO. 2320-5407

Journal homepage: <http://www.journalijar.com>

INTERNATIONAL JOURNAL
OF ADVANCED RESEARCH

RESEARCH ARTICLE

Resistive switching in the Al/Si/SiO₂/CdS/Polymer/Al structure fabricated at room temperature

Luqman Sufer Ali¹ and Ahmed Waled kasim²

1. University of Mosul/Department of Electrical Engineering

2. Technical College of Mosul/Department of Computer Technology.

Manuscript Info

Manuscript History:

Received: 15 June 2015

Final Accepted: 19 July 2015

Published Online: August 2015

Key words:

*Corresponding Author

Luqman Sufer Ali

Abstract

Resistance random access memory (RRAM), which uses a resistive switching phenomenon found in transition metal oxides. A RRAM memory cell is a capacitor-like structure composed of insulating or semiconducting transition metal oxides that exhibits reversible resistive switching on applying voltage pulses. CdS and Polymer (Cellulose Acetate) – based RRAM possessing stable resistive switching is investigated in this work. A new structure of a memory was investigated. It is constructed with silicon as a substrate and silicon oxide thermally grown on it and active materials that consist of CdS layer as a semiconductor n-type and Polymer (Cellulose Acetate) layer sandwiched between the two electrode using same metal. The Polymer layer are coating by using Spin-Coater Instrument. The present structure is behaving as unipolar resistive switching because this structure can be switched between high - resistance state (HRS) and low - resistance state(LRS). The top electrode area will affect on the resistive behavior also. This effect is occurred more in large top electrode area ($TE_L=15.896\text{mm}^2$) where , the forming voltage (V_{forming}) are inversely proportional with respect to the top electrode area (A).also, the (HRS) inversely proportional with the (A).Finally, the resistance ratio (R_{ratio}) are directly proportional with the(A).The compliance current ($I_{\text{cc}}=25\text{mA}$) are used for protecting the device from the damage. The fabricated structure has many prosperities , such as $V_{\text{forming}} = 6.2\text{volt}$ at $I=7.7\text{mA}$, $V_{\text{set}} = 2.85\text{volt}$, $V_{\text{Reset}} = 1.4\text{volt}$ and $R_{\text{ratio}}=16.28$.

Copy Right, IJAR, 2015,. All rights reserved

INTRODUCTION

Due to the intense demand for a high-density, high-speed, and low-power nonvolatile memory (NVM) in semiconductor industry, the market of NVM has grown much faster than the entire semiconductor market in recent years [1]. As a traditional NVM, Si-based Flash memory has been extensively applied in mobile storage for its relatively high density and low fabrication cost [2]. Nevertheless, Flash suffers from several disadvantages such as low endurance, low speed and high voltages in the write operation, and it is rapidly approaching its fundamental scaling limit due to the increasing difficulty of retaining electrons in shrinking dimensions[1], [3]. Therefore, new materials and novel device architectures are proposed to overcome this technical and physical scaling limit.

There are various candidates competing with each other for the next-generation memory. For example, magnetic random access memory (MRAM) and ferroelectric random access memory (FRAM), which use magnetic tunnel junctions and reversible polarization of ferroelectric materials, respectively, and have attracted numerous attention and enjoyed advanced development [4] . However, MRAM and FRAM both face severe problems in scaling [1] , [

3]. Under this circumstance, a new candidate emerged: resistance switching random access memory (RRAM), in which the memory cells have the theoretical smallest area $4F^2$ (F is the feature size on a given process)[5].

Resistive switching phenomenon was firstly reported in a series of binary oxides by Hickmott in 1962[6]. Since then, the hysteretic resistive switching behavior under the applied electric field has been reported in many materials [7]. Hence, the first period of high research activity of resistive switching phenomenon had arisen in 1970s and 1980s. Most of the early researches focused on discussing and revealing the physical mechanism of electrical stimulated resistive switching. As the development of microelectronics processing technology, researchers recognized that resistive switching behavior has the potential to be utilized as an ultimate NVM in the late 1990s, bringing the second research surge of resistive switching [8]. So far, a great variety of materials have been found to show the resistive switching characteristics, including binary oxides such as NiO, TiO₂, and ZnO, solid electrolytes such as Ag₂S, GeSe, perovskites, organic materials, amorphous silicon (α -Si), and nitrides [9].

Most of the RRAM cells have a simple capacitor-like 'MIM' structure, as shown in Figure(1), where 'M' denotes a kind of metal electrode as well as electro-conducting non-metals, and 'I' stands for an insulator or semiconductor layer sandwiched by two electrodes. Because of its simple structure, an attractive architecture named crossbar memory structure has been proposed, which offers the highest possible device density and the simplest interconnect configuration. As shown in Figure(2), each cross-point between Word line and Bit line becomes a storage cell. Thus, the cell size of the memory can be diminished to nanoscale by using nanowires as the orthogonal crossbar. This configuration also provides potential three-dimensional (3D) storage by multilevel stacking the Word and Bit lines. Although RRAM has attracted scientific and commercial interests as well as numerous experimental researches, the switching mechanism is still debating. Different switching behaviors such as unipolar phenomenon and bipolar phenomenon, various switching mechanisms such as filament model, trap controlled model, interface barrier model and Mott transition are involved in RRAM researches[9].

II. CLASSIFICATION OF RESISTIVE SWITCHING :

II.1 UNIPOLAR AND BIPOLAR RESISTIVE SWITCHING BEHAVIORS:

The basic characteristic of RRAM is its two different resistance states, i.e. high resistance state (HRS) and low resistance state (LRS), which can be switched from one to the other by an appropriate electric stimulus. In general, the operation which changes the resistance of the device from HRS to LRS is called a 'SET' process, while the opposite process is defined as 'RESET'. The specific resistance state (HRS or LRS) can be retained after the electric stress is cancelled, which indicates the nonvolatile nature of RRAM. The resistances of HRS and LRS can be read at a small voltage, which does not affect the resistance state. According to the relationship of electrical polarity between SET and RESET processes, the resistive switching behaviors can be simply divided into two kinds: unipolar and bipolar, which manifest different current - voltage ($I-V$) appearances, as shown in Figure(3)(a) and (b), respectively.

In unipolar RRAM, the switching direction does not depend on the polarity of the applied voltage. Figure (3)(a) depicts the typical $I-V$ curves of the unipolar resistive switching. As it can be seen, the device switches from HRS to LRS at a high voltage (VSET). Subsequently, the system returns to HRS at a voltage (VRESET) lower than VSET. In the SET process, a current compliance (I_{cc}) is often used to avoid permanent breakdown, while it is unnecessary to apply I_{cc} in RESET process. Devices which exhibit the unipolar $I-V$ characteristic often have the symmetric structure, which means that the top electrode (TE) using the same material as the bottom electrode (BE). This type of resistive switching behavior has often been observed in binary oxide system, such as Pt/TiO₂/Pt, Pt/ZnO/Pt, Pt/NiO/Pt and Al/ZrO₂/Al. The switching mechanism of the unipolar RRAM is ascribed that the conducting filament forming under voltage stimulus puts the device into LRS and Joule heating effect caused filament rupture switches it back to HRS. Since the Joule heating effect does not depend on the polarity of the current, this kind of devices displays unipolar switching behavior.

In contrast, the switching direction of bipolar RRAM depends on the polarity of the applied voltage, as depicted in Figure(3)(b). The polarity of VRESET is opposite to that of VSET, and LRS (HRS) is not affected by the electrical signal whose polarity is identical with that of VSET (VRESET). The device structure of bipolar switching is usually asymmetric. For example, different materials are used as TE and BE. A big problem in unipolar resistive switching is that VSET may overlap with VRESET owing to the same polarity of VSET and VRESET. Apparently, this kind of trouble does not exist in bipolar resistive switching since the reversed polarity of voltage in SET and RESET processes. Bipolar RRAM has extensively investigated by aiming to prepare the nonvolatile switches in

reconfigurable large-scale integrated circuits (LSIs). Some different mechanisms are involved in bipolar switching RRAM, which leads to various switching characteristics. I_{cc} may be avoided in some circumstances [9].

II.II FILAMENT-TYPE AND INTERFACE-TYPE MECHANISMS IN RESISTIVE SWITCHING :

The mechanisms of resistive switching can be divided by the conduction mode in LRS: the filament type and the interface type, as shown in figure (4). In the filamentary resistive switching, current in LRS flows through the confined local path in the insulating matrix while current in HRS flows through the films homogeneously. Although the filamentary conducting path has been demonstrated in many systems, the constitution of filament seems vary from one to another. Metallic nano-bridges, oxygen vacancies (VO^{2+} s) composed conductive channels, dislocations and a trail of metallic islands are possible filaments which switch the device to LRS. A distinct feature of filament-type resistive switching is that the resistance in LRS (RLRS) is independent on device area while the resistance in HRS (RHRS) increases when the cell size decreases. In addition, the confirmed filamentary mechanism specifies a direction to scale devices, since the size of the filament determines the ultimate scaling limit. Leastwise, the device size should be double of the size of the filament[9].

In the interface type resistive switching, the current which flows through the film is determined by the barrier height at the interface between the middle semiconductor layer and the electrode. The interface barrier height can be modified by electrical stimuli, and lead to two different resistance states. This type of resistive switching has been observed in complex perovskites oxides and binary oxides. YANG et al[11] reported the resistive switching in Ti/TiO₂/Pt system, where TiO₂/Ti contact is Ohmic and TiO₂/Pt interface is Schottky-like. Negative voltage on Pt electrode drifts V_o toward the TiO₂/Pt interface and reduces the barrier height, resulting in the resistive switching from HRS to LRS and vice versa. In perovskites, a mechanism concerning the charging effect at the interface is also proposed to explain the resistive switching. The distribution of trapped charge is altered by the voltage stresses in forward or reverse directions, resulting in the modification of band lineup or tunneling probability in the interface barrier. Similarly, Mott transition induced by carriers doped at the interface can be classified into interface type resistive switching. The interface barrier height is an identical factor although it can be altered in different ways[9].

Migration of electronic and/or optical functions that have been performed in inorganic materials to organic materials is an exciting direction for chemists and materials scientists. RRAM based on organic materials has attracts many interests during the last decades due to the advantages of low cost, rich structure flexibility and easy – fabrication [12]. In 1968, GREGOR[13],observed resistive switching effect in sandwich structure of Pb/poly(divinylbenzene)/Pb, which was among the earliest reports about organic RRAM. Since then, resistive switching effect has been reported in a great number of traditional polymers and small organic molecules with metal/organic layer/metal sandwich structure such as Al/poly(N-vinylcarbazole) (PVK)/Al[14],Al/pentacene/Al[15] and Al/8-hydroxyquinoline aluminum/Au [16]. Recently, some new organic materials have been synthesized and found to have resistive switching effect with the structure of ITO/organic layer/Al. FAZZI et al[17] reported that a new class of relatively flexible conjugated molecule which belongs to diphenyl - bithiophene derivatives displayed electrical bistability. KUOROSAWA et al[18] successfully synthesized two new triphenylamine based polyimides, which showed potential for high performance memory devices. In addition, active researches have also been focused on the combination of functional components with organic layers and many interesting phenomena have been observed. For example, blending different content of carbon nanotube in PVK is capable of exhibiting different device behaviors. Also, organic RRAM devices composed of Ag nanoparticles embedded in a polymethyl methacrylate were fabricated and presented current bistability.

More than four decades have passed since the first report about organic RRAM. But, the understanding of relevant resistive switching mechanism in any given organic RRAM device is still a topic of active debate[12]. It has been widely proposed that the resistive switching of organic RRAM is governed by SCLC and localized filament mechanism. In LRS, localized current paths have been observed by CAFM in several systems, but the essence of the current paths has not been clearly identified. A metallic bridge connecting the two electrodes, of course, is the simplest form of filament[12], just as in the inorganic RRAM systems. However, the current paths created by local alignment of the middle organic layer were also studied by some groups[19], such as ITO/poly-3,4-ethylenedioxythiophene : poly-styrenesulfon ate (PEDOT:PSS)/Al system. In addition, the efficiency of the electrons and/or holes injection at the electrode/organic interface and the charge transport across the organic materials might be responsible for the low and high resistance states and the resistive switching between them[12],[17].

Recently, COLLE et al[20] found that the existing of a thin aluminum oxide was essential for the resistive switching rather than the middle organic layer, which challenges the preceding observations. Thus, complete

understanding of the relevant resistive switching mechanism in organic RRAM is still an open question. Apart from the switching mechanism, some criteria must be met for the real application. Compared with the inorganic RRAM, the RRAM based on organic materials is in an unfavorable position in terms of speed to write and read, cycling endurance, retention time and power

consumption according to the current progress. There is still a long way to go to advance organic RRAM into practical applications of benefit to society. More studies need to be focused on identifying the switching mechanism and fabricating RRAM devices with better performance rather than creating new materials, which can keep the organic RRAM to be closer to real application.

IV. EXPERIMENTS :

To construct the present structure, the wafer of silicon p-type $\langle 100 \rangle$ is used as a substrate and prepared using special cleaning process. The second step after cleaning the substrate is the oxidation using a furnace with maximum temperature (1000°C) to make thermal oxidation of thickness (75 \AA) see figure (4). The next step after thermal oxidation is the depositing a thin layer of Cadmium Sulfide CdS with thickness (750 \AA) by using the thermal evaporation system (the Balzer system). The CdS thin film here represents n-type semiconductor. Before the final step, the Spin-Coater Instrument type (INSTRAS, sck-100 spin coater kit) are used to coating a thin layer of Polymer (Cellulose Acetate) on the CdS layer with thickness about 1500 \AA . The final step for fabrication of the structure is the depositing thin layers of metal (Al) with thickness of (2000 \AA) as Top Electrodes (TES) for three areas (15.896 mm^2 , 4.906 mm^2 and 3.14 mm^2) on the Polymer (Cellulose Acetate) layer by using special masks see figure (5). The bottom electrode is fabricated by depositing (Al) metal of (2000 \AA) on the other face of the wafer see figure (6). The structures are tested with AC and DC sources using maximum current of ($I_{cc} = 25 \text{ mA}$) as compliance current.

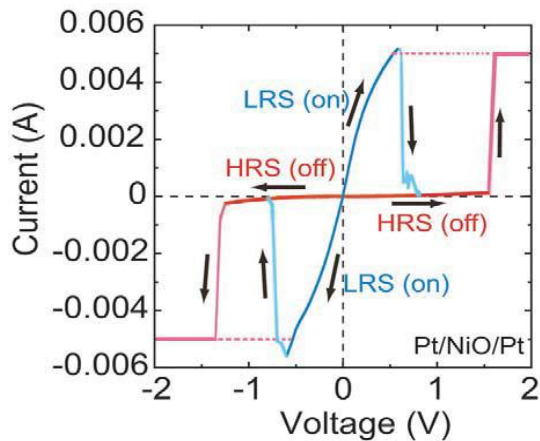
V. RESULTS AND DISCUSSION:

V.I. Testing the Devices using DC measurements:

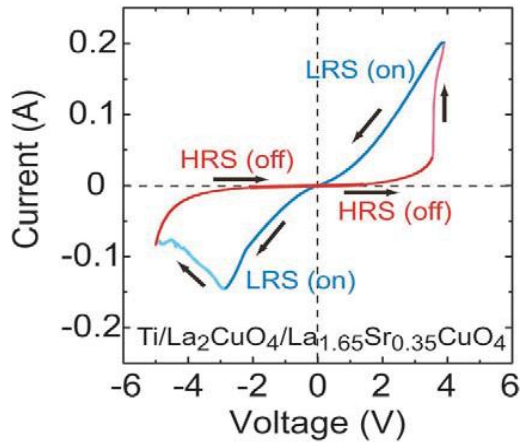
The DC testing of memory can be achieved by using (I-V) characteristics of the fabricated device were measured by (KEITHLEY 6487 PICOAMMETER / VOLTAGE SOURCE) for three states:

- With large Top Electrode (TEL), The area is $A_L = 15.896 \text{ mm}^2$.
- With medium Top Electrode (TE_m), The area is $A_m = 4.906 \text{ mm}^2$.
- With Small Top Electrode (TES), The area is $A_s = 3.14 \text{ mm}^2$.

Through the result of DC (I-V) characteristics, Appears that the symmetry with respect to the origin for two bias of positive and negative voltage are equal, So, the positive bias will be enough for studying the resistive switching of the device as shown in the figure (7).

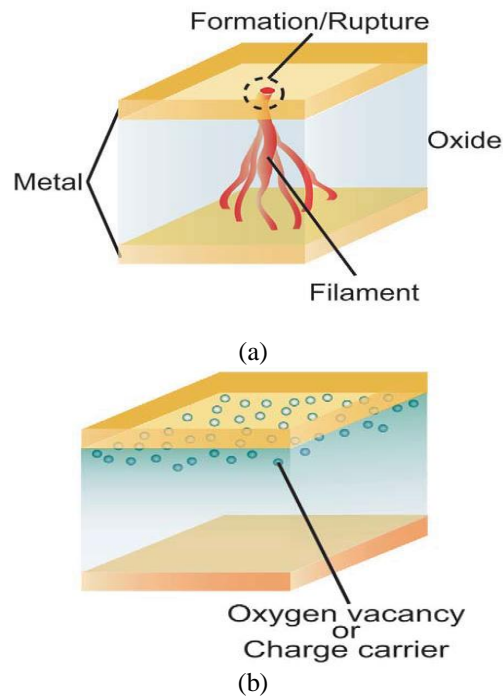


(a)



(b)

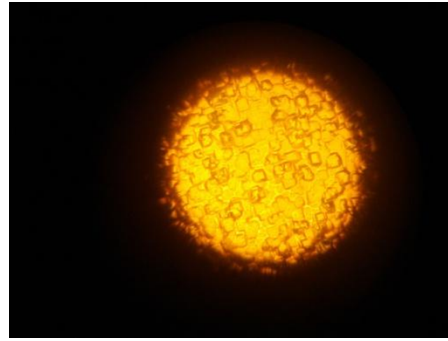
Figure (3) (I - V) curves for (a) unipolar (nonpolar) switching in a Pt/NiO/Pt cell and (b) bipolar switching in a Ti/La₂CuO₄/La_{1.65}Sr_{0.35}CuO₄ cell. In unipolar switching, the switching direction depends on the amplitude of the applied voltage. Bipolar switching shows directional resistance switching according to the polarity of the applied voltage[10].



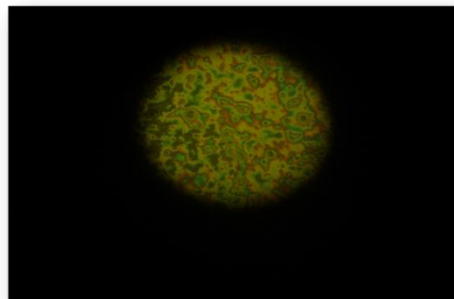
(b)

Figure (4) Proposed models for resistive switching can be classified according to either (a) a filamentary conducting path, or (b) an interface-type conducting path [10].

III. RESISTIVE SWITCHING IN ORGANIC MATERIALS:



(a)



(b)

Figure (4) The image of the Metal - Microscope with amplification by 600 for the internal composition of the p-type silicon (sample) (a) before the thermal oxidation (b) after the thermal oxidation with $SiO_2=75\text{\AA}$. [This image taking by the Metal – Microscope type UNION with amplification by 600 in Technical Institute in Mosul].

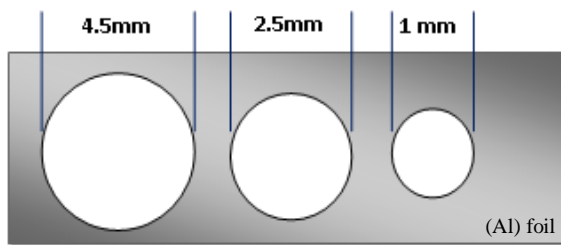


Figure (5) the mask shape for fabricated structure.

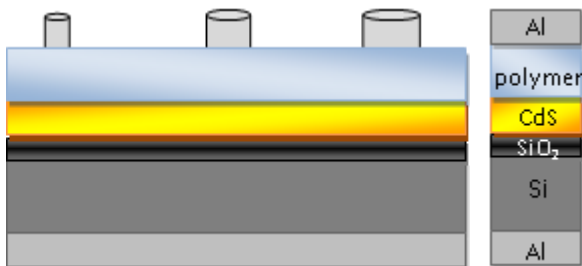


Figure (6) the cross section of the structure.

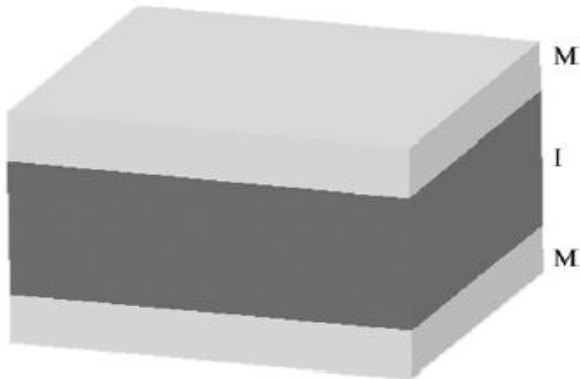


Figure (1) A schematic diagram of simple capacitor-like ‘MIM’ structure of a single RRAM cell[9].

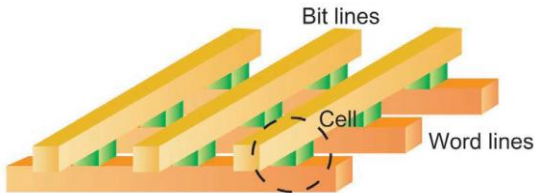


Figure (2) Configuration of a crossbar memory structure (Every cross-point between Word lines and Bit lines serves as a storage cell) [10].

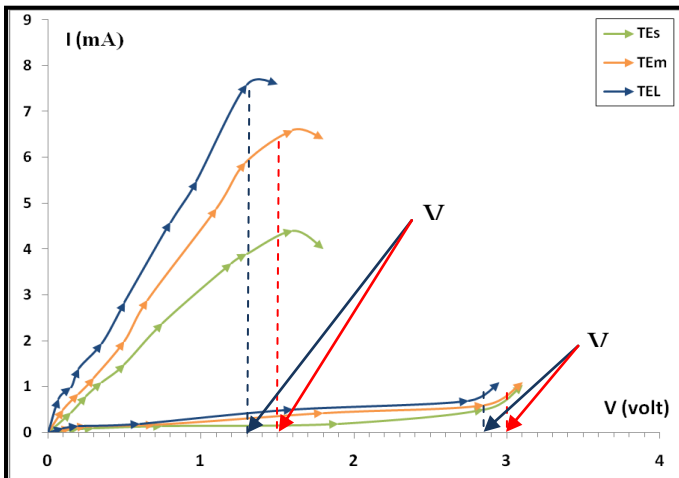


Figure (7) (I-V) characteristics for the device with Polymer coating (Cellulose Acetate) for many electrodes areas using compliance current $I_{cc}=25mA$.

From above figure ,the values of voltages ($V_{forming}$, V_{set} , V_{Reset} and low resistance switching (RLRS)) in case of TES will be higher than those values in case of TEM and TEL respectively. While the resistance of the device in case of high resistance switching (RHRS) are inversely proportional with changing of the area of top electrode, this congruently with conclusions the researcher Seo and et al. , for resistive switching [21].Finally, the compliance current (I_{cc}) are used for protection the device from damaging , So, this equal to $I_{cc}=25mA$.Table (1-1) summarizes the changing of this above values.

The above Structures behave Unipolar resistive switching. This may happen because the structure uses the same material (Al) as top and bottom electrodes [22].

TE _L			TE _m					TE _s		
V _{Reset}	R _{HRS}	R _{LRS}	V _{forming}	V _{set}	V _{Reset}	R _{HRS}	R _{LRS}	V _{forming}	V _{set}	V _{Reset}
1.4 V	3 KΩ	KΩ 0.18	6.5V	3V	1.6V	3.75 KΩ	0.24 KΩ	6.6V	3V	1.6V

Table (1-1) summary for the important measured parameters for the device with Polymer coating (Cellulose Acetate) for many tops electrodes areas.

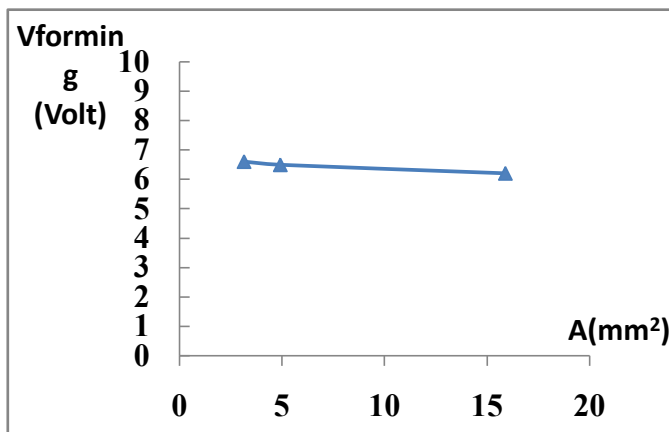
From table (1-1) , the resistance ratio

$$(R_{ratio}=R_{HRS}/R_{LRS}) \text{ can be calculated for many electrodes areas and summarizing in table (1-2).}$$

Table (1-2) R_{ratio} for many devices with Polymer coating (Cellulose Acetate) for many tops electrodes areas.

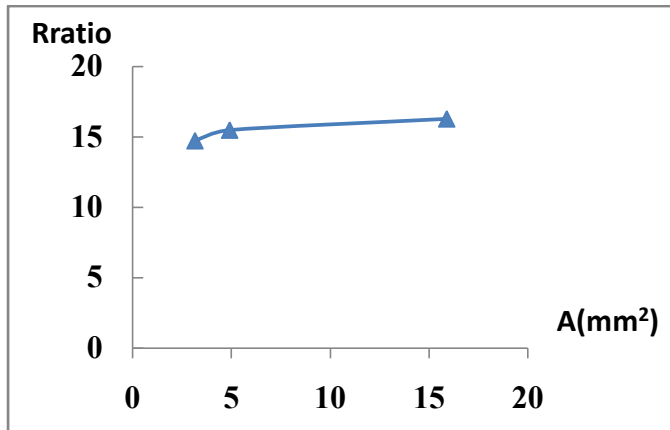
R _{ratio}		
TE _L	TE _m	TE _s
16.28	15.47	14.73

From table (1-1), there are present inversely proportional between the top electrode area (A) with forming voltage V_{forming} for each device. So, this relation can be drawing as shown in figure (8).



Figure(8) The relation between A and V_{forming} for many devices with Polymer coating (Cellulose Acetate).

From table (1-2) , there are direct relation between A and R_{ratio} for many devices with Polymer coating (Cellulose Acetate) as shown in figure (9).



Figure(9) The relation between A and R_{ratio} for many devices with Polymer coating (Cellulose Acetate).

The resistor endurance of the device with Polymer coating (Cellulose Acetate) in case of TEL was studied as shown in figure (10). From this figure ,there are one order of magnitude between low resistance state(LRS) and high resistance state (HRS).

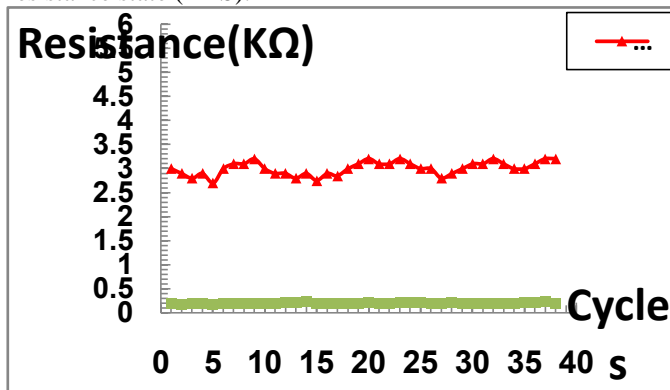


Figure (10) Endurance for resistance LRS and HRS of the device with Polymer coating (Cellulose Acetate) in case of TEL.

In same manner, the voltage endurance(V_{set} and V_{Reset}) of the device with Polymer coating (Cellulose Acetate) in case of TEL can be achieved as shown in figure(11).

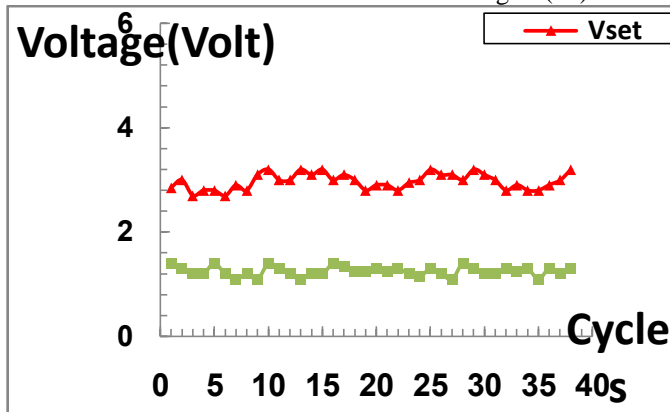


Figure (11) Endurance of the voltages(V_{set} and V_{Reset}) of the device with Polymer coating (Cellulose Acetate) in case of TEL.

V.II. Testing the Devices using AC Measurements:

The AC testing of memory can be achieved, by using (I-V) characteristics of the fabricated devices. The measurements were fulfilled using Storage Digital Oscilloscope type (OWON MSO 7102T) and Function Generator type (PHILIPS PM 5127 0.01Hz – 1MHz) giving a triangle pulses.

From AC testing, the following can be determined:

1) Resistance Ratio Measurement (R_{ratio}):

These measurements can be achieved by the drawing between (I-V) for the device under test (DUT), where channel 1 (ch1) represented the voltage across DUT and channel 2 (ch2) represented the current through DUT by dividing the voltage across DUT on $R=100\Omega$. So, figure (12) and figure (13) represent the AC measurements in case of TEL and in case of TEM respectively.

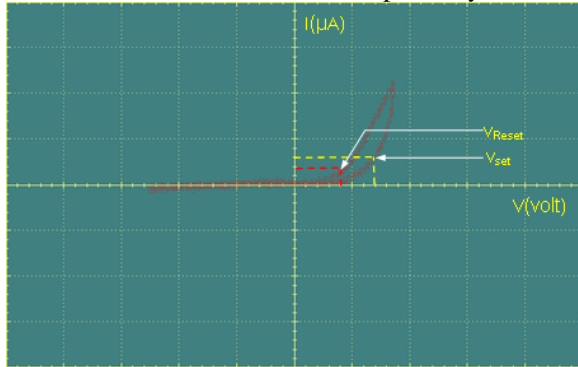


Figure (12) the AC measurements of the device with Polymer coating (Cellulose Acetate) in case of TEL (these measurements were taken by using Storage Digital Oscilloscope type (OWON MSO 7102T)).

So, in case of TEL the R_{ratio} is calculated as:

$$R_{HRS} = R_{off} = \frac{1.4 \times 2 V}{0.6 \times 2 mA} = \frac{2.8 V}{1.2 mA} = 2.33 K\Omega$$

$$R_{LRS} = R_{on} = \frac{0.8 \times 2 V}{0.4 \times 20 mA} = \frac{1.6 V}{8 mA} = 0.2 K\Omega$$

$$R_{ratio} = \frac{R_{HRS}}{R_{LRS}} = \frac{R_{off}}{R_{on}} = \frac{2.33 K\Omega}{0.2 K\Omega} = 11.65$$

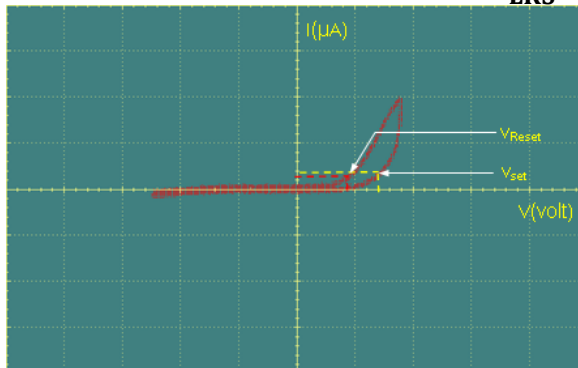


Figure (13) the AC measurements of the device with Polymer coating (Cellulose Acetate) in case of TEM (these measurements were taken by using Storage Digital Oscilloscope type (OWON MSO 7102T)).

So, in case of TEM the R_{ratio} is calculated as:

$$R_{HRS} = R_{off} = \frac{1.4 \times 2 V}{0.4 \times 2 mA} = \frac{2.8 V}{0.8 mA} = 3.5 K\Omega$$

$$R_{LRS} = R_{on} = \frac{0.9 \times 2 V}{0.3 \times 20 mA} = \frac{1.8 V}{6 mA} = 0.3 K\Omega$$

$$R_{ratio} = \frac{R_{HRS}}{R_{LRS}} = \frac{R_{off}}{R_{on}} = \frac{3.5 K\Omega}{0.3 K\Omega} = 11.66$$

One can be observed that The values of the parameters R_{HRS} , R_{LRS} , R_{ratio} , V_{set} and V_{Reset} in AC measurements are nearly equal to DC measurements of the device with Polymer coating (Cellulose Acetate) in case of TEL and TEM.

2) Switching Time Measurement (T_s):

By AC measurements, the Switching Time Measurement (T_s) of the device with Polymer coating (Cellulose Acetate) can be calculated in case of TEL and TEM respectively.

So, from figure (12) the Switching Time is calculated as:

$$T_s = \frac{1}{f_s} = \frac{1}{4.755\text{kHz}} = 210.3 \mu\text{s}$$

And from figure (13) the Switching Time is calculated as:

$$T_s = \frac{1}{f_s} = \frac{1}{4.277\text{kHz}} = 233.8 \mu\text{s}$$

V.III. Scanning electron microscope (SEM) Measurements:

A scanning electron microscope (SEM) is a type of electron microscope that produces images of a sample by scanning it with a focused beam of electrons. The electrons interact with atoms in the sample, producing various signals that can be detected and that contain information about the sample's surface topography and composition. The electron beam is generally scanned in a raster scan pattern, and the beam's position is combined with the detected signal to produce an image. SEM can achieve resolution for less than 1 nanometer. Samples can be observed in high vacuum, in low vacuum, and (in environmental SEM) in wet conditions. The SEM measurement for the device with Polymer coating (Cellulose Acetate) is achieved at the Nanotechnology and Advance Materials Research Center in University of Technology in Baghdad, see figure(14).

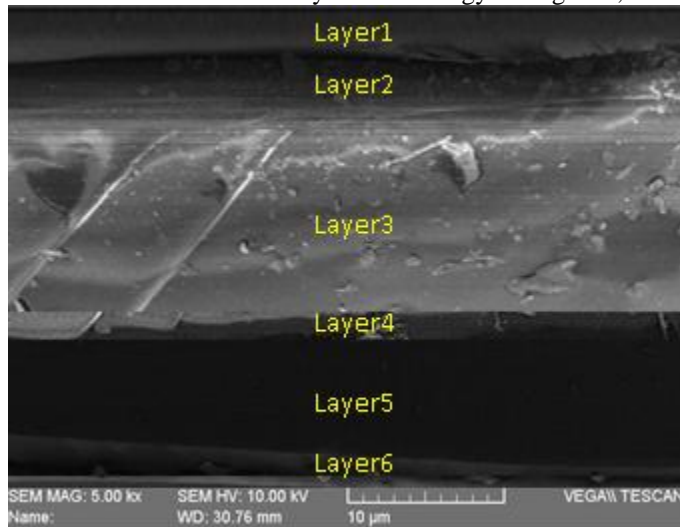


Figure (14) Cross - sectional scanning electron microscopy (SEM) images for the device with Polymer coating (Cellulose Acetate).[This image is taken by (SEM) underling the Nanotechnology and Advance Materials Research Center in University of Technology in Baghdad].

The SEM image (figure 14) reveals six layers. Layers (1 and 6) represent the top and bottom metal electrodes (Al) respectively, while layers (5 and 4) represent the cross section silicon wafer and the silicon oxide which is grow thermally on the silicon substrate ,while the layer (3) is the active martial CdS which represents the n-type semiconductor deposited on the silicon oxide, finally the layer (2) represents the Polymer martial (Cellulose Acetate).

VI. CONCLUSIONS :

From the discussion above, it can be concluded that the resistive - switching mechanisms of RRAM device can be distinguished through the (I – V) relations, in two cases , DC and AC . The device exhibits the Unipolar (I – V) characteristics , because has symmetric structure, which means that the top electrode (TE) using the same material as the bottom electrode (BE) (Al). From the experiments , it is clear that the resistance in high resistive state HRS is inversely proportional to the area of the TE. That is to say $V_{forming}$, V_{set} and V_{Reset} for the same structure will change. also, the forming voltage($V_{forming}$) is inversely proportional with respect to the top electrode area (A) , this may occur because availability of a local filamentary conducting paths within the zone of this area. also, this represents the same reason which leading to make the Switching Time(T_s) to be inversely proportional with respect to the top electrode area(A).Finally, the resistance ratio (R_{ratio}) is directly proportional with the (A). The fabricated structure has many prosperities , such as $V_{forming} = 6.2\text{volt}$ at $I = 7.7\text{mA}$, $V_{set} = 2.85\text{volt}$, $V_{Reset} = 1.4\text{volt}$ and $R_{ratio} = 16.28$.

ACKNOWLEDGEMENTS :

We are deeply thankful to the Electrical Engineering Department in the University of Mosul, in addition to the Technical Institute of Mosul and the Nanotechnology and Advance Materials Research Center in Baghdad.

REFERENCES :

- [1] G. I. MEIJER, “Materials science—Who wins the nonvolatile memory race? ”, *J. Science* ,Vol. 319(5870),p. 1625–1626,2008.
- [2] A. FLOCKE, T. G. NOLL, C. KUGELER, et al. “A fundamental analysis of nano-crossbars with non-linear switching materials and its impact on TiO₂ as a resistive layer. ”, In: 8th IEEE Conference on Nanotechnology (NANO) [J]. Arlington, USA, p. 319–322,2008.
- [3] A. SAWA, “Resistive switching in transition metal oxides”, [J]. *Mater Today*, vol. 11(6), p. 28–36 ,2008.
- [4] S.S.P. PARKIN, K.P. ROCHE, M.G. SAMANT, et al., “Exchange-biased magnetic tunnel junctions and application to nonvolatile magnetic random access memory”, *J Appl Phys* ,vol. 85(8), p.5828–5833,1999.
- [5] W. W. ZHUANG, W. PAN, B. D. ULRICH, et al., “Novell colossal magnetoresistive thin film nonvolatile resistance random access memory (RRAM) ”, *International Electron Devices Meeting, Technical Digest. San Francisco* ,p. 193–196,2002.
- [6] T. W. HICKMOTT, “Low-frequency negative resistance in thin anodic oxide films”, *J Appl Phys*, vol. 33(9) , p. 2669–2682,1962.
- [7] G. DEARNALE, et al. “Electrical phenomena in amorphous oxide films”, *Rep Prog Phys*, vol. 33(11), p. 1129–1191, 1970.
- [8] A . ASAMITSU, Y . TOMIOKA, H . KUWAHARA, et al., “ Current switching of resistive states in magnetoresistive manganites”, *J. Nature* , vol. 388(6637), p.50–52 ,1997.
- [9] P. Feng, et al., “Nonvolatile resistive switching memories-characteristics, mechanisms and challenges ”,*Progress in Natural Science: Materials International* ,vol. 20 , p. 01-15, 2010.
- [10] A. Sawa , “Resistive switching in transition metal oxides”, *materialstoday*, vol.11(6), p. 28-36, 2008.
- [11] J. J. YANG, M. D. PICKETT, M. LI X, et al., “ Memristive switching mechanism for metal/oxide/metal nanodevices”, *Nat Nanotechnol* , vol. 3(7), p. 429–433, 2008.
- [12] J. C. SCOTT and L. D. BOZANO, “ Nonvolatile memory elements based on organic materials”, *Adv Mater*, vol. 19(11) , p. 1452–1463, 2007.
- [13] V. GREGOR L, “ Polymer dielectric films”, *IBM J Res Dev*, vol. 12(2) , p. 140–162 , 1968.
- [14] S. LAI Y, C. H. TU, D. L. KWONG, et al., “ Bistable resistance switching of poly(N-vinylcarbazole) films for nonvolatile memory applications”, *Appl Phys Lett* , vol. 87(12) , p. 122101, 2005.
- [15] D. TONDELIER, K . LMIMOUNI, D .VUILLAUME, et al., “ Metal/organic/metal bistable memory devices”, *Appl Phys Lett* , vol. 85(23) , p. 5763–5765, 2004.
- [16] A. K. MAHAPATRO, et al., “ Electric-field-induced conductance transition in 8-hydroxyquinoline aluminum (Alq3) ”, *J Appl Phys* , vol. 96(6), p. 3583–3585, 2004.

- [17] D. FAZZI, C. CASTIGLIONI, F. NEGRI, et al., “ Structure and electrical bistability of a new class of diphenyl-bithiophenes: a combined theoretical and experimental study”, *J Phys Chem C*, vol. 112 (47), p. 18628–18637, 2008.
- [18] T. KUOROSAWA, C. C. CHUEH, C. L. LIU, et al., “ High performance volatile polymeric memory devices based on novel triphenylamine-based polyimides containing mono- or dual-mediated phenoxy linkages”, *Macromolecules*, vol. 43(3) , p. 1236–1344, 2010.
- [19] X. H. LIU, Z. Y. JI, D. Y. TU, et al., “ Organic nonpolar nonvolatile resistive switching in poly(3,4-ethylene-dioxythiophene):polystyrenesulfonate thin film ”, *Org Electron*, vol. 10(6) , p.1191–1194, 2009.
- [20] M. COLLE ,et al., “ Switching and filamentary conduction in non-volatile organic memories”, *Org Electron*, vol. 7(5), p. 305–312, 2006.
- [21] S. Seo, W. Je, A. Hw, "Electrode dependence of resistance switching in polycrystalline NiO Films", *Appl. Phys. Lett.*, vol.87, p.263507.
- [22] P. Feng, C. Chao, et al., “ Nonvolatile resistive switching memories-characteristics, mechanisms and challenges”, Laboratory of Advanced Materials, Department of Materials Science and Engineering, Tsinghua University, Beijing 100084, China.